Desorption-induced fragmentation of silica aggregates

T. Narayanan,* J.-M. Petit,† M. L. Broide,‡ and D. Beysens§
Service de Physique de l'Etat Condensé, Commissariat à l'Energie Atomique, Centre d'Etudes Nucleaires de Saclay, Orme des Merisiers, F91191 Gif-sur-Yvette Cedex, France
(Received 19 December 1994)

We have studied the dynamics of fragmentation of colloidal silica aggregates in a binary mixture of 2,6-lutidine and water. Here, the aggregation is caused by a temperature dependent adsorption process and the fragmentation is initiated by quenching the suspension below the aggregation temperature. Using small angle light scattering, we have deduced the evolution of mean cluster mass (M) and radius of gyration (R) of the clusters during the course of breakup. We find that M and R exhibit a power law decay for shallow quenches and exponential decay for deep quenches. In terms of the scaling description of linear fragmentation, the above finding corresponds to the kernel index changing from 1 to 0 as the quench depth is increased.

PACS number(s): 68.45.Da, 05.40.+j, 82.70.Dd

Fragmentation is a complex phenomenon, involved in many natural processes such as the crushing of rocks, polymer degradation, breakup of liquid droplets, etc. Recently, this phenomenon has received considerable attention as a sequel to the developments in the complimentary process of aggregation [1–4]. There has been considerable progress in developing a scaling theory of fragmentation using a system of linear rate equations [1–4]. However, the complexity of this phenomenon restricted a parallel advancement of the experimental endeavors [5].

In this paper, we present an experimental system in which the fragmentation is driven by a temperature dependent desorption process. The system consists of colloidal silica dispersed in a binary mixture of 2,6-lutidine (L) and water (W). This charge stabilized suspension aggregates as a result of the strong adsorption of lutidine onto the colloids when the bulk coexistence temperature of the host mixture is approached [6]. The aggregation occurs above a specific temperature (T_a) and is reversible in character. The reversible nature of the aggregation allowed us to probe the dynamics of fragmentation very quantitatively.

The kinetics of aggregation of silica spheres in LW has been studied recently [7]. The main findings are (i) the structure factor obeys Porod's law and is approximately a square Lorentzian in qR, where q is the scattering wave vector and R is the mean radius of gyration of the aggregates, and (ii) the mean cluster mass and mean radius of gyration evolve with time (t) as t and $t^{1/3}$, respectively, suggesting that the clusters have a compact, nonfractal geometry and that the individual spheres in the aggregate are enveloped in a L rich phase.

We performed extensive small angle light scattering measurements on two samples (A and B). One of them (A) was the same sample A investigated in Ref. [7] and the results reported in this paper are obtained from this sample. The sample B was prepared using silica spheres of the same diameter ($=346$ nm that were filtered through millipore filters of pore diameter 0.8 μm). Sample B also yielded identical results. The samples were prepared using L (Merck, filtered through millipore filters of diameter $=0.22$ μm) and W obtained from a Milli-Q system. The weight fractions of the silica spheres and L were the same (0.0015 and 0.20, respectively) in both samples. The mixtures were contained in high quality optical cells with a path length of 2 mm. The experimental setup used was similar to that employed in Ref. [7]. The temperature of the water bath was varied rapidly by circulating hot or cold water as the case may be. The rapid changes in the bath temperature were recorded by means of a calibrated thermistor contained in a cell identical to that used for the samples and located at an equivalent thermal point. Typical equilibration time for temperature quenches up to 60 mK was about 20 s.

The angular distribution of the scattered intensity was measured for scattering angles between 0.7° and 13.6° corresponding to a q range of 1.7×10^5 m^{-1} $<q<3.2\times10^6$ m^{-1}. The incident intensity was provided by a He-Ne laser of power of about 5 mW. The scattered light from the sample cell was collimated onto a viewing screen by a plano-convex lens of focal length 17.5 cm. The transmitted beam was turned by 90° by means of a minute prism that was stuck in front of a beam stop at the center of the lens. The intensity distribution on the screen was recorded by an eight-bit video camera. The transmitted and incident laser intensities were also measured simultaneously. The image was digitized and the azimuthal average of the scattered intensity as a function of q was computed. Further corrections were applied for the background intensity, the dark count of the camera,

*Present address: Physics Department, Oklahoma State University, Stillwater, OK 74078. Electronic address: narayan@vms.ucc.okstate.edu
†Electronic address: jmpetit@amoco.saclay.cea.fr
‡Present address: Physics Department, Lewis and Clark College, Portland, OR 97219. Electronic address: broide@lclark.edu
§Electronic address: beysens@amoco.saclay.cea.fr

 ©1995 The American Physical Society

sample turbidity, and the form factor of the unaggregated spheres.

In each experiment, the scattered intensity was recorded prior to aggregation (10 mK below T_a). Aggregation was then initiated by rapidly heating the bath about 60 mK above T_a. As the aggregation proceeded, the bath temperature was lowered to 25 mK above T_a in order to facilitate a more controlled quench to the stable region. When the transmission reached a value corresponding to R_g of about 1.5 μm[longer times (>500 s) were highly undesirable due to possible perturbations by gravity], the bath temperature was lowered rapidly below T_a to the desired temperature $T_{\exp}$. The scattered intensity was recorded before and during the course of fragmentation. In each experiment, the time at which the quench was initiated is taken as the starting time ($t=0$) and the onset of fragmentation is indicated by the rapid increase in the transmitted intensity. Typical fragmentation time t_f (time required for the transmitted intensity to reach its value before aggregation) varied from 20 to 600 s, depending upon the quench depth ($\Delta T=T_a-T_{\exp}$), and it decreased with ΔT. Furthermore, it was necessary to quench the sample appreciably below T_a (12 mK for sample A) to produce complete fragmentation, i.e., recover the same transmitted intensity as that before aggregation. In addition, the recovery of the same transmitted intensity before aggregation verified that gravitational settling of the clusters was negligible.

Figure 1(a) displays the diminishing of scattered intensity $I(q)$ for a $\Delta T=17$ mK. As in the case of aggregation [7], we find that $I(q)$ over the measured range of q can be fitted to the following expression:

$$I(q)=I(0)/[1+(qR_g)^2/3\alpha]^{\alpha}\ , \tag{1}$$

where $I(0)$ and R_g are proportional to the mean cluster mass (M) and radius of gyration (R), respectively. The continuous lines in Fig. 1(a) are generated using Eq. (1) for $\alpha=2$. It is evident from Fig. 1(a) that Eq. (1) adequately describes all the $I(q)$ data, which suggests that the cluster structure is nearly preserved during the breakup process.

The scaling predictions [1] concerning the decay rate of M and R are based mainly on the continuum model, which assumes that both M and R vanish as $t\to\infty$. Whereas in the experiment, the fragmentation terminates at finite values [corresponding to the $I(q)$ of the unaggregated suspension] of $I(0)$ and R_g^2. Hence, to make a direct comparison of the decay rates of $I(0)$ and R_g with the theory, we subtracted the final (unaggregated) values of $I(0)$ and R_g^2 (I_m and R_m^2, respectively) from their values deduced using Eq. (1) during the breakup process. These reduced quantities are denoted by I_f [$=I(0)-I_m(0)$] and R_f^2 ($=R_g^2-R_m^2$) and they represent M and R^2, respectively. Over the q range of our measurements, I_m and R_m^2 differ considerably from that corresponding to the form factor of unaggregated spheres. Gurfein, Beysens, and Perrot [8] also noticed this departure for $q<10^7$ m^{-1} and they attributed this feature as being due to either the interactions between spheres or the permanent aggregates present in the system. However, we found that R_m is nearly reproducible from sample to sample (A and B) and hence we assert that the large value of R_m (four times the sphere radius) is a result of the interactions in the system. This is also the conclusion reached by Philipse and Vrij [9] in a study involving charged silica spheres suspended in ethanol, where they found that the measured value of the second virial coefficient corresponds to an effective hard sphere diameter of about 4.5 times the single sphere diameter—suggesting the presence of interparticle interactions extending over several sphere radii [9].

Figure 1(b) depicts the decay of I_f and R_f^3 with time. One of the striking features of this graph is the time lag between the onset of decrease of I_f and R_f^3 (and hence M

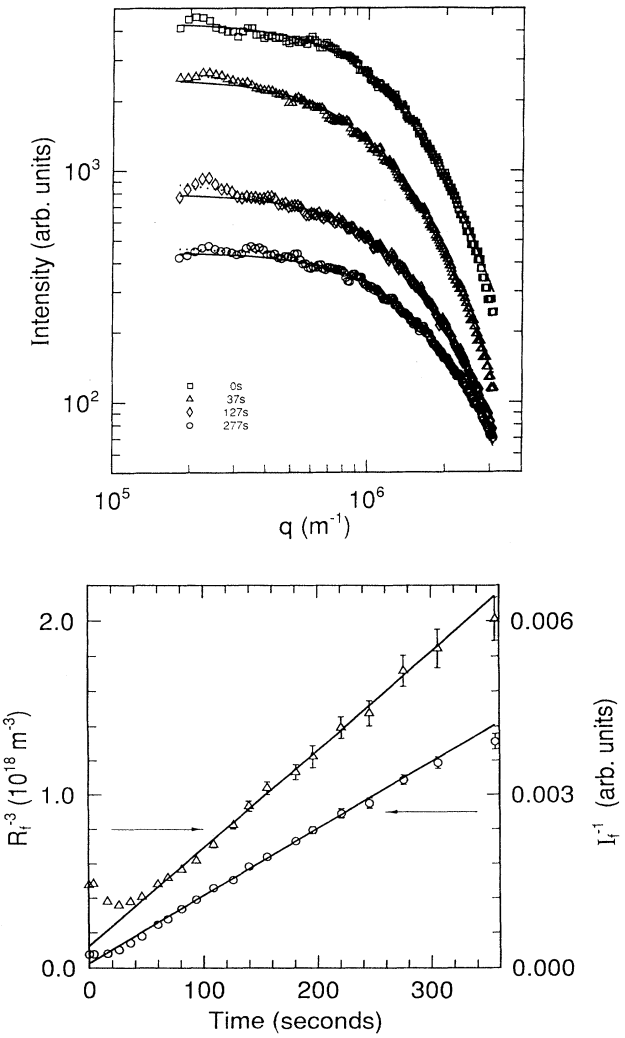

FIG. 1. (a) Evolution of scattered intensity for a ΔT of 17 mK. Continuous lines are generated using Eq. (1) and dotted lines using Eq. (2). (b) Time dependence of parameters I_f and R_f^3 (see text) for the above fragmentation experiment ($I_m=132$ and $R_m=5.6\times10^{-7}$ m). Continuous lines correspond to $I_f^{-1}=7.73\times10^{-5}+1.17\times10^{-5}t$ (arbitrary units) and $R_f^{-3}=(0.14+0.0055t)10^{18}$ m^{-3} and demonstrate the power law decay of I_f and R_f^3. Initial dip in R_f^{-3} manifests a marginal increase in the cluster size prior to breakup.

and R^3). The initial dip in R_f^{-3} indicates that the clusters "inflate" before they actually disintegrate. This suggests that the desorption of L, which precedes fragmentation permits the monomers in the cluster to diffuse away leading to an increase in cluster diameter. At the latter times, it is clear from Fig. 1(b) that I_f and R_f^3 decay by a power law in t with an exponent of unity. The linear time dependence of I_f and R_f^3 also establishes the compact nature of the fragments. It should be mentioned that the power law decay of M and R can be shown, directly (without reducing to I_f and R_f), in a plot of $I(0)$ and R_g^3 vs reciprocal of time.

We have also investigated the kinetics of fragmentation for deeper quenches. The choice of final temperature was limited by the time required for the sample to equilibrate. The diminishing of $I(q)$ for a relatively deeper quench ($\Delta T = 33$ mK) is illustrated in Fig. 2(a). At the latter stage of fragmentation, $I(q)$ deviates from Eq. (1) and is marked by the appearance of an intense peak at $q = 0$. While attempting to rationalize the occurrence of this additional intensity, we examined the possibility of a change in aggregate structure during the course of breakup. In other words, when L is desorbed from the clusters, the individual sphere positions become visible, possibly leading to fragments assuming fractal geometry. In that case α in Eq. (1) becomes equal to $d_f/2$, where d_f is the fractal

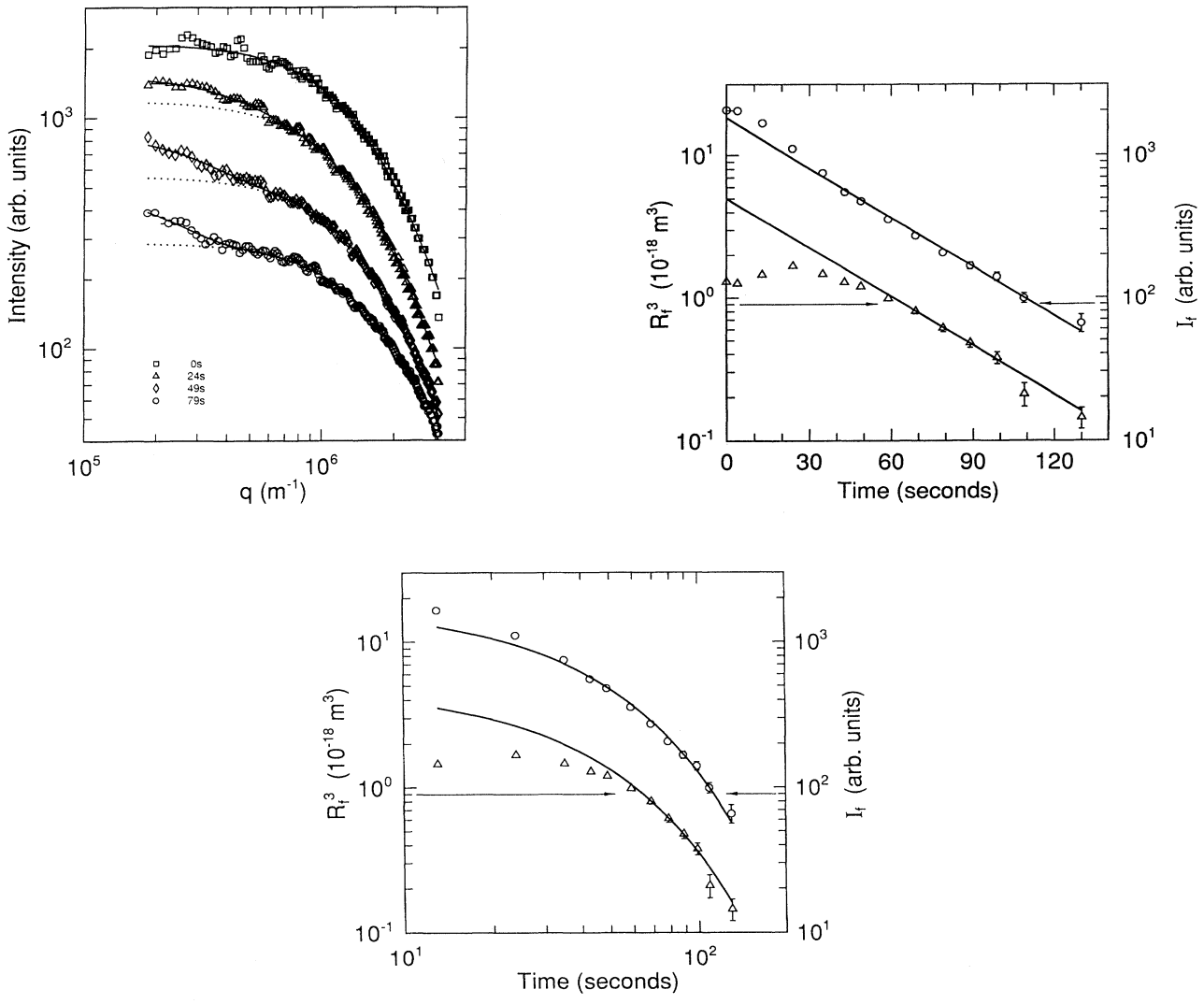

FIG. 2. (a) Evolution of scattered intensity for $\Delta T = 33$ mK. The solid curves are generated using Eq. (2) and the dotted lines refer to $I_p = 0$ in Eq. (2). (b) Time variant of parameters I_f and R_f^3 for the above fragmentation experiment ($I_m = 81$ and $R_m = 5.8 \times 10^{-7}$ m). The solid lines pertain to $I_f = 1796 \exp(-0.0265t)$ (arbitrary units) and $R_f^3 = (5.01 \times 10^{-18}) \exp(-0.0265t)$ m^3, reveal the exponential decay of I_f and R_f. Small deviation of I_f from the fitted line at the early stages is attributed to the time taken for the initiation of the process. (c) Comparison in a log-log scale between power law decay and exponential law decay for the time variation of parameters I_f and R_f^3 for the above fragmentation experiment ($I_m = 81$ and $R_m = 5.8 \times 10^{-7}$ m).

dimensionality. However, we found that the lowering of α alone did not result in a satisfactory fit to the very late time $I(q)$ data. Moreover, R_g^2 deduced in this manner increased with time, which seemed unphysical. We also attempted to incorporate an additional Lorentzian term with an adjustable linewidth and intensity, in Eq. (1), which again was found to be inadequate to fit the data over the entire range of time. Eventually, we recognized that Eq. (1) with an additive Gaussian term could satisfactorily describe all the data. The final expression used to fit the data in Fig. 2(a) has the following form:

$$I(q)=I(0)/[1+(qR_g)^2/6]^2+I_p\exp(-q^2R_p^2)\ , \qquad (2)$$

where I_p and R_p are additional fitting parameters. The continuous lines in Fig. 2(a) are generated by the above expression.

Equation (2) is identical to the form of $I(q)$ used by Debye, Anderson, and Brumberger in the analysis of small angle x-ray scattering from porous materials [10]. They ascribed the first term (square Lorentzian) to the correlation (characterized by an exponential correlation function) between holes of random shape and size in the solid and the second term to the correlation between larger inhomogeneous regions (of correlation radius R_p) in the material. In the present case, we attribute the Gaussian term as due to the correlation between bare silica spheres that are produced at a faster rate when the fragmentation rate is large. However, it should be recognized that the weight of the Gaussian term is significant only at small q's ($<7\times10^5$ m^{-1}) and reliable estimates of $I(0)$ and R_g^2 can be obtained graphically from an $I(q)^{-1/2}$ vs q^2 plot. The dotted lines in Fig. 2(a) correspond to Eq. (2) for $I_p=0$. Towards the completion of the breakup process (60 s for Fig. 2 data), the central peak disappears (resulting in $I_p=0$) and R_p attains about 5 μm, which is close to the intersphere distance in the stable suspension.

Figure 2(b) displays the time dependence of parameters I_f and R_f. As in the case of slow fragmentation, there exists a finite time lag between the onset of decay of I_f and R_f^3 and during this intervening period R_f (and hence R_g) increases marginally. The straight line in Fig. 2(b) for I_f corresponds to $I_f=1796\exp(-0.0265t)$ (arbitrary units) and demonstrates an exponential decay of I_f, in contrast to the power law decay of I_f that has been observed for $\Delta T=17$ mK [Fig. 1(b)]. A power law fit with an arbitrary exponent to the I_f data (33 mK) yielded larger deviations than the exponential fit. This is clearly shown in a log-log scale [Fig. 2(c)]. In addition, the decay rate of R_f^3 is consistent with the behavior of I_f as indicated by the straight line [in Fig. 2(b)] that corresponds to $R_f^3=5.01\times10^{-18}\exp(-0.0265t)$ m^3.

In order to explain the two distinct scenarios (exponential and power law decay of M and R), we describe the breakup process in terms of the linear fragmentation rate equation [1–4]

$$\frac{dc(x,t)}{dt}=-a(x)c(x,t)+\int_x^\infty c(y,t)a(y)f(x/y)dy\ , \qquad (3)$$

where $c(x,t0$ and $c(y,t)$ are the concentration of particles of diameter x and y, respectively, $a(x)$ and $a(y)$ are the corresponding overall rates of breakup, and $f(x/y)$ is the rate at which x is produced from the breakup of y. This rate equation is valid irrespective of the actual mechanism underlying the breakup process. The cluster mass distribution satisfies the following scaling ansatz [1]:

$$c(x,t)=M^{-2}\phi(x/M)\ , \qquad (4)$$

where M is the typical cluster mass and $\phi(x/M)$ is the scaled cluster size distribution. For homogeneous reaction kernels $a(x)=x^\lambda$, where λ is the homogeneity index of the kernel, Eqs. (3) and (4) yield the following scaling relations [1]:

$$M=[\lambda wt+M(0)^{-\lambda}]^{-1/\lambda} \quad \text{for } \lambda\neq0\ , \qquad (5a)$$

$$M=M(0)\exp(-wt) \quad \text{for } \lambda=0\ , \qquad (5b)$$

where w is the separation constant (>0) proportional to the average number of fragments [1] and $M(0)$ is the initial mean cluster mass. The results presented in Figs. 1(b) and 2(b) thus supports $\lambda=1$ for slow fragmentation and $\lambda=0$ for fast fragmentation. Evidently, λ is dependent on the quench depth.

Physically, $\lambda=1$ implies that all bonds in a cluster are equally scissionable and $\lambda=0$ indicates that all clusters break with equal probability regardless of their size [4]. The latter case ($\lambda=0$) can have significant implications in light scattering experiments because when all clusters fragment at the same rate, there will be an accumulation of larger clusters in the system towards the completion of the breakup process and these larger fragments can dominate the scattering at small **q**'s. The Gaussian term in Eq. (2) may be a direct consequence of the presence of these larger clusters, which are in some sense analogous to *inhomogeneities* in the language of Debye, Anderson, and Brumberger [10]. In slow fragmentation ($\lambda=1$), the Gaussian term is either nonexistent or insignificant as indicated by the dotted lines in Fig. 1(a), which are generated by the fit to Eq. (2).

As shown in Ref. [11], two limiting cases of fragmentation ($\lambda=1$ and $\lambda=0$) can be understood in terms of the time required for the various subprocesses involved in the breakup process. When ΔT is small, the fragmentation is governed by the rate of desorption of L from the clusters, and for large ΔT the breakup process is limited by the time required for the Brownian diffusion of colloids [11].

We have investigated the dynamics of fragmentation for different ΔT's (from 12 to 53 mK). We find that $\lambda=1.0(\pm0.25)$ for ΔT's up to 28 mK and $\lambda=0$ for ΔT's above 32 mK, manifesting a rapid change in the λ value in the vicinity of 28 to 32 mK. The exact switching temperature is a sample dependent parameter (as is T_a). At the moment, we are not in a position to comment upon the kinetics of fragmentation for very deep quenches ($\Delta T>50$ mK) because the fragmentation time is too short (<30 s) to acquire equilibrated data, and the Gaussian term in Eq. (2) rapidly dominates the scattering. For very deep quenches ($\Delta T>50$ mK), there could be a shattering transition ($\lambda<0$) in which smaller clusters break at faster rates resulting in the rapid production of

monomers [1–4]. This scenario merits a separate scrutiny.

In conclusion, the dynamics of fragmentation of silica colloids in the binary mixture of 2,6-lutidine+water obeys the scaling predictions of linear fragmentation. We have identified two separate fragmentation regimes where the average cluster mass decays with time either exponentially or by a power law (with an exponent close to unity).

This work was partially supported by the Indo-French Centre for Promotion of Advanced Research and the Centre National d'Etudes Spatiales. We thank M. Bonetti, F. Perrot, C. Allain, and M. Cloitre for useful discussions.

[1] Z. Cheng and S. Redner, Phys. Rev. Lett. **60**, 2450 (1988); J. Phys. A **23**, 1233 (1990).

[2] E.D. McGrady and R. M. Ziff, Phys. Rev. Lett. **58**, 892 (1987).

[3] B. F. Edwards, M. Cai, and H. Han, Phys. Rev. A **41**, 5755 (1990).

[4] R. M. Ziff and E. D. McGrady, Macromolecules **19**, 2513 (1986); J. Phys. A **18**, 3027 (1985).

[5] L. Ouali and E. Pefferkorn, J. Colloid Interface Sci. **161**, 237 (1993).

[6] D. Beysens and D. Esteve, Phys. Rev. Lett. **54**, 2123 (1985).

[7] M. L. Broide, Y. Garrabos, and D. Beysens, Phys. Rev. E **47**, 3768 (1993), and references therein.

[8] V. Gurfein, D. Beysens, and F. Perrot, Phys. Rev. A **40**, 2543 (1989).

[9] A. P. Philipse and A. Vrij, J. Chem. Phys. **88**, 6459 (1988); see also the recent study in a similar system by M. L. Kurnaz and J. V. Maher, Phys. Rev. E (to be published).

[10] P. Debye, H. R. Anderson, Jr., and H. Brumberger, J. Appl. Phys. **28**, 679 (1957); for an alternate explanation of the Lorentzian-squared structure factor, see P. Wong, J. W. Cable, and P. Dimon, J. Appl. Phys. **55**, 2377 (1984).

[11] J. M. Petit, T. Narayanan, M. L. Broide, and D. Beysens, in *Proceedings of Workshop on Fragmentation Phenomena, Les Houches, 1993,* edited by D. Beysens, X. Campi, E. Pefferkorn (World Scientific, Singapore, 1995).